JOURNAL OF PHYSICS AND CHEMISTRY

CSK SCIENTIFIC PRESS

Review Article
Volume 2 | issue 3

Enhancing Geological Interpretation with Seismic Attributes in Fuba Field, Onshore Niger Delta, Nigeria

U Ochoma

Department of Physics, Rivers State University, P.M.B 5080, Port Harcourt Nigeria

*Corresponding Author: U Ochoma, Department of Physics, Rivers State University, P.M.B 5080, Port Harcourt Nigeria

Submitted: 15 Mar 2024 **Accepted:** 20 Mar 2024 **Published:** 29 Mar 2024

Citation: *U Ochoma (2024). Enhancing Geological Interpretation with Seismic Attributes in Fuba Field, Onshore Niger Delta, Nigeria J of Physics & Chemistry, 2(3), 1-8.*

Abstract

Enhancing geological interpretation with seismic attributes in Fuba Field, Onshore Niger Delta, Nigeria using Well-log and 3D Seismic data are here presented. Seismic interpretation was carried out using Petrel software. The structural interpretation of seismic data reveal highly synthetic and antithetic faults which are in line with faults trends identified in the Niger Delta. Of the 36 interpreted faults, only synthetic and antithetic faults are regional, running from the top to bottom across the field. These faults play significant roles in trap formation at the upper, middle and lower sections of the field. Three distinct horizons were mapped. Fault and horizon interpretation reveal closures which are collapsed crestal structures bounded by these two major faults. The depth structure maps reveal anticlinal faults. For a comprehensive analysis of the structural and stratigraphic understanding of the reservoirs, six seismic attributes variance edge, chaos, dip magnitude, sweetness, root mean square and spectral decomposition were applied to the seismic data. The variance and chaos values range from 0.0 to 1.0. The dip magnitude values range from 0 to 90 degrees. The Variance edge, chaos and dip magnitude analysis were used to delineate the prominent and subtle faults in the area. The sweetness value ranges from 0 to 22,500. The RMS amplitude values range from 0 to 13,000 in the reservoirs The RMS amplitude and sweetness results highlighted the hydrocarbon zones. The results of spectral decomposition indicate areas of low frequency and high amplitude associated with known hydrocarbon zones and the presence of small-scale faults, channels and lobes in the field. The result of the seismic attribute analysis has shown that Fuba field has good hydrocarbon prospects.

Keywords: Seismic Attributes, Growth Faults, Chaos, Sweetness, Spectral Decomposition, Niger Delta, Nigeria.

Introduction

Seismic attributes are quantities of geometric, kinematic, dynamic, or statistical features obtained from seismic data [1-3]. Subsurface quantitative interpretations require seismic attributes to supplement conventional seismic reflection amplitudes [4]. Structural and stratigraphic traps could be very subtle and are therefore difficult to map accurately[5]. The geometrical attributes are used for structural and stratigraphic interpretations of seismic data [6]. It is therefore possible to use seismic attribute to map geological features such as faults [7]. Seismic attributes describe reservoir properties by giving derivatives of quantities extracted from the seismic data to relate the seismic wave's event directly or indirectly to geology [8]. Seismic attributes are used in most seismic exploration and reservoir study to correctly image the subsurface geological structures, correctly characterize the amplitudes of the seismic data and to obtain information on reservoir properties [9-11]. Improved methodologies are needed to discriminate between true hydrocarbon indicators and non-indicators by imaging the detailed subsurface structure with a view to delineate new hydrocarbon zones that might be hidden in structural traps for the development programmes of the field. Seismic attributes analysis being an integral part of 3D seismic interpretation is one of these advancements [12] Several researchers have made enormous contributions based on seismic attributes for enhanced structural and stratigraphic interpretations within the Niger Delta basin to investigate the potentiality of hydrocarbon deposits [13-14]. Ochoma, 2023 analyzed the relevant seismic attributes such as variance edge, root mean square, maximum amplitude, average magnitude and maximum magnitude applied to the seismic data. The variance values ranges from 0.0 to 1.0. The Variance edge analysis was used to delineate the prominent and subtle faults in the area. The RMS amplitude values ranges from 9,000 to 13,000 in the reservoirs. The root mean square amplitude, maximum amplitude, average magnitude and maximum magnitude analysis reveal bright spot anomaly. These amplitude anomalies served as direct hydrocarbon indicators (DHIs), unravelling the presence and possible hydrocarbon prospective zones. Results from this study showed that away from the currently producing zone of the field, additional leads and prospects exist, which could be further evaluated for hydrocarbon production. Ayolabi and Adigun, (2013) delineated six hydrocarbon bearing zones from well logs and estimated their petrophysical parameters[14]. The trapping mechanism identified from their interpretation indicates that the field is characterized mostly by fault assisted closures and a few four way closures. Thus, where conventional seismic interpretation has failed, seismic attributes analysis complement.

This study is taken from Fuba Field, Onshore, Niger Delta, Nigeria. The ultimate deliverable of this study was enhancing geological interpretation using 3-D seismic attributes analysis in the area. The major components of our study are: (a) Well Correlation performed in order to determine the continuity of the reservoir sand across the field. (b) Seismic Interpretation which involves well-to-seismic tie, fault mapping, horizon mapping, time surface generation and generation of seismic attributes. This aids in giving more insight into enhancing geological interpretation using 3-D seismic attributes analysis.

Location and Geology of the Study Area

The proposed study area Fuba Field is located in the onshore Niger Delta region. Figure 1 shows the map of the Niger Delta region showing the study area while Figure 2 shows the base map showing well locations in the study area. The Niger Delta lies between latitudes 4° N and 6° N and longitudes 3° E and 9° E [15]. The Delta ranks as one of the major oils and gas provinces globally, with an estimated ultimate recovery of 40 billion barrels of oil and 40 trillion cubic feet of gas[16]. The coastal sedimentary basin of Nigeria has been the scene of three depositional cycles [17]. The first began with a marine incursion in the middle Cretaceous and was terminated by a mild folding phase in Santonian time. The second included the growth of a proto-Niger delta during the Late Cretaceous and ended in a major Paleocene marine transgression. The third cycle, from Eocene to Recent, marked the continuous growth of the main Niger delta. A new threefold lithostratigraphic subdivision is introduced for the Niger delta subsurface, comprising an upper sandy Benin Formation, an intervening unit of alternating sandstone and shale named the Agbada Formation, and a lower shaly Akata Formation. These three units extend across the whole delta and each range in age from early Tertiary to Recent. They are related to the present outcrops and environments of deposition. A separate member of the Benin Formation is recognized in the Port Harcourt area. It is Miocene-Recent in age with a minimum thickness of more than 6,000ft (1829m) and made up of continental sands and sandstones (>90%) with few shale intercalations [18]. Subsurface structures are described as resulting from movement under the influence of gravity and their distribution is related to growth stages of the delta [19]. Rollover anticlines in front of growth faults form the main objectives of oil exploration, the hydrocarbons being found in sandstone reservoirs of the Agbada Formation. The oil in geological structures in the basin may be trapped in dip closures or against a synthetic or antithetic fault.

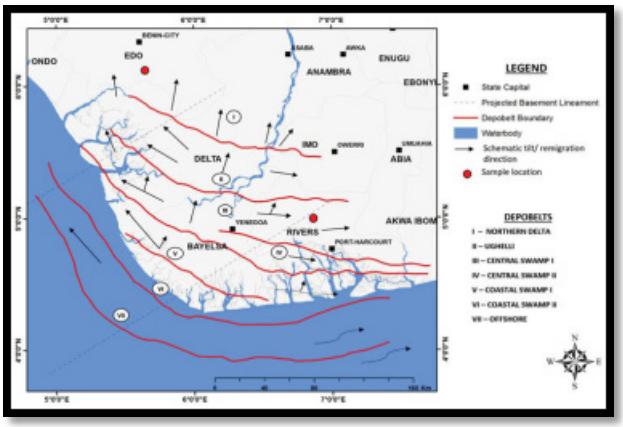

Figure 1: Map of Niger Delta Showing the study Area

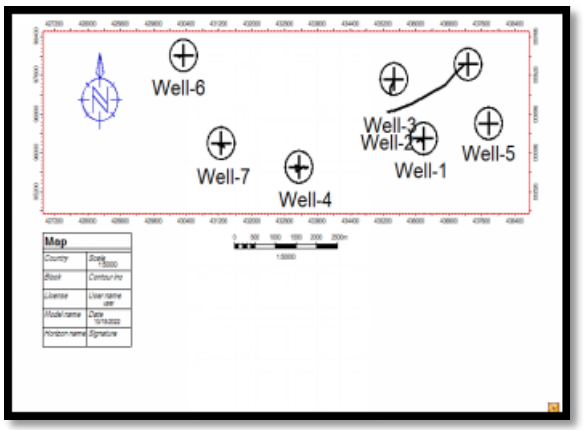

Figure 2: Base Map of Showing Well Locations in the Study Area

3.0 Materials and Methods

3.1 Well-to-Seismic Ties

Well correlation is the first stage of the pre-interpretation process. The process of well correlation involves lithologic description, picking top and base of sand-bodies, fluid discrimination and then linking these properties from one well to another based on similarity in trends. In between these two lithologies in the subsurface, the gamma ray log is often used. Correlation of reservoir sands was achieved using the top and base of reservoir sands picked. The correlation process was possible based on similarity in the behaviour of the gamma ray log the Niger Delta; the predominant lithologies are sands and shales. In order to discriminate shapes. Also, the thickness of the shale bodies overlying and underlying the sand body is considered during Correlation. After defining the lithologies, the resistivity log was used for discriminating the type of fluid occurring within the pores in the rocks.

There are five basic steps involved in seismic interpretation relevant to this study and they include; Well-to-seismic ties, Fault Mapping, Horizon mapping, Time surface generation and Attributes generation. Well-to-seismic tie is a process that enables the visualization of well information on seismic data. For this process to be achieved, the following are basic requirements; checkshot, sonic log, density log and a wavelet. The sonic log, which is the reciprocal of velocity, was calibrated using the checkshot data. The calibration process is necessary in order to improve the quality of the sonic log because the sonic log is prone to washouts and other wellbore related issues. The results of calibrating the sonic log with the checkshot gives a new log called the calibrated sonic log.

The calibrated sonic log is used along with the density log to generate an acoustic impedance (AI) log. The acoustic impedance log is calculated for each layer of rock. The next step in-

volves generating the reflectivity coefficient (RC) log. The RC is calculated and generated using the AI log. The RC log generated is then convolved with a wavelet to generate a synthetic seismogram which is comparable with the seismic data. The extended white 2 wavelet utilized for convolution is extracted from the seismic data. The synthetic seismogram was generated. The mathematical expressions that govern the entire well-to-seismic tie workflow are presented below:

$$AI = \rho v \quad (1)$$

$$RC = \frac{\rho_2 v_2 - \rho_1 v_1}{\rho_2 v_2 + \rho_1 v_1} \quad (2)$$

$$\text{Synthetic Seismogram} = \frac{\rho_2 v_2 - \rho_1 v_1}{\rho_2 v_2 + \rho_1 v_1} * wavelet \quad (3)$$

where AI = acoustic impedance, RC = reflection coefficient, = density; v = velocity.
Faults were identified as discontinuities or breaks in the seismic reflections. Faults were mapped on both inline and cross-line directions. Horizons are continuous lateral reflection events that are truncated by fault lines. The horizon interpretation process was conducted along both inline and crossline direction. At the end of the horizon mapping, a seed grid is generated which serves as an input for time surface generation. Time surfaces were generated using the seed grids gotten from the horizon mapping process.

Among the seismic attributes that have been used in the visualization of the geology of the subsurface are variance, chaos, dip magnitude, sweetness, root mean square amplitude and spectral decomposition. The seismic volume attributes analysis was applied to the seismic inline 8515 while the root mean square amplitude was generated as surface attribute.

3.2: Variance (Edge Detection) Method

In the Petrel software, the variance attribute uses an algorithm that computes the local variance of the seismic data through a multi-trace window with user-defined size. The local variance is computed from horizontal sub-slices for each voxel. A vertical window was used for smoothing the computed variance and the observed amplitude normalized. The variance attribute measures the horizontal continuity of the amplitude that is the amplitude difference of the individual traces from their mean value within a gliding CMP window.

$$\sigma^2 = \frac{1}{n}\sum_{f_i=1}^{n}(x_i + x_m)^2 \quad (4)$$

Where $\sigma =$ standard deviation, $\sigma^2 =$ variance, n = the number of observations, f_i frequency x_i = the variable, x_m = mean of x_i.

3.3: Chaos

Chaos attribute is defined as a measure of the "lack of organization" in the dip and azimuth estimation method. It can be used to distinguish different sediment facies in lithology variation environments (for example, sand and shale).

3.4: Dip Magnitude

Dip magnitude is analogous to strike and dip of sedimentary layers. The dip magnitude is defined as the angle between the steepest direction of a plane and a horizontal plane, where values range from 0 to 90. The dip magnitude attribute computation in Petrel software makes use of the inbuilt formula:

$$\text{True dip} = \tan^{-1}\left(\frac{\tan(\theta_y)}{\tan(\beta_x)}\right) \quad (5)$$

where Θ_y = apparent dip in a direction (y) and β_x dip azimuth relative to a direction (x).
Dip magnitude is a good attribute, not only for showing overall structure folds, but can be used to identify faults with very small displacement.

3.5: Determination of Sweetness

Sweetness involves the implementation of envelopes and instantaneous frequency that are combined. Mathematically, it is expressed as

$$S(t) = \frac{\alpha(t)}{\sqrt{f_\alpha(t)}} \quad (6)$$

where S(t) = Sweetness, α(t) = Envelope, f_α(t) = instantaneous frequency.
Sweetness is used for the identification of features where the total energy signatures change in the seismic data.

3.6: Determination of Root Mean Square (Rms) Amplitude

The root mean square (RMS) amplitude was extracted from the seismic data as a surface attribute. Root mean square (RMS) amplitude is used to obtain a scaled estimate of seismic trace envelope. It is obtained in the software by sliding a tapered window of N samples as the square root of the sum of all the trace value x squared. The RMS attribute computation in Petrel software makes use of the inbuilt formula:

$$X_{rms} = \sqrt{\frac{1}{N}\sum_{n=1}^{N} w_n x_n^2} \quad (7)$$

where X_{rms} = root mean square amplitude, W_n = window values, N = number of samples in the window, x = trace value.

3.7: Spectral Decomposition

Spectral decomposition is a frequency attribute. It involves separating and classifying seismic events within each trace based on their frequency content. Each 1D trace was decomposed from the time domain into its corresponding 2D representation in the time-frequency domain using algorithms. Once each trace was transformed into the time-frequency domain, a band-pass filter was applied to view the amplitude of seismic data at different frequencies.

The short-time Fourier transform (STFT) spectrogram which is the squared modulus of the STFT and the spectral energy density is defined as [20].

$$SP_s(t,f) = /\int_{-\infty}^{\infty} s(\tau)h(\tau - t)e^{-j2\pi f\tau}d\tau /^2 \qquad (8)$$

Where, $h(\tau - t) =$ the window function, $s(\tau) =$ the signal, SP_s = the short-time Fourier transform
j = the imaginary unit, $\tau =$ the time delay.
The relationships between the amplitude spectrum ($A(w)$) and the phase spectrum ($\gamma(w)$) of the estimated transformed signals are presented in equations 8 and 9

$$/A(\omega^T)/ = \sqrt{A_r + A_i} \qquad (9)$$

$$\gamma(\omega) = \mathrm{Tan}^{-1}[\frac{A_i}{A_r}] \qquad (10)$$

A_r = real part of $A(\omega^T)$, A_i = imaginary part of $A(\omega^T)$, frequency, T = transform of the signal and $A(\omega^T)$ = amplitude of transformed trace at frequency ω.

4.0: Results and Discussion

4.1: Reservoir Identification and Correlation

The results for lithology and reservoir identification are presented in Figure 3. A total of four sand bodies (L, M, N and O) were identified and correlated across all seven wells in the field. Three reservoir sands were selected for the purpose of this study (M, N and O). The resistivity logs which reveals the presence of hydrocarbons were used to identify the hydrocarbon bearing sands. On Figure 3, the sands are coloured yellow while shales are grey in colour.

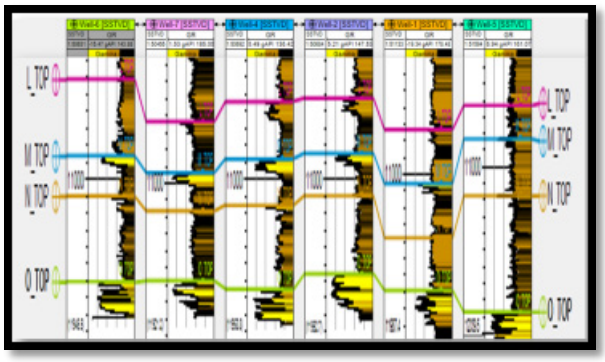

Figure 3: Well section showing reservoir identified and correlated across Fuba Field

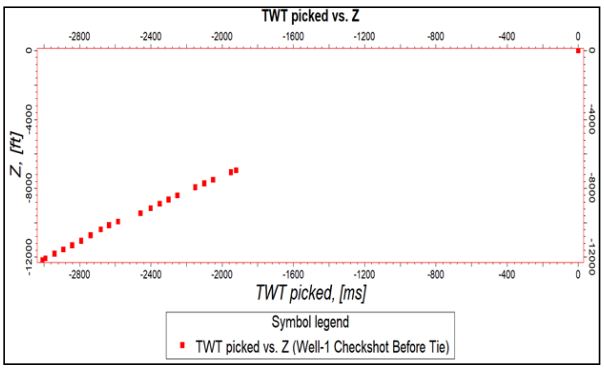

Figure 4: Checkshot Quality for Well-1

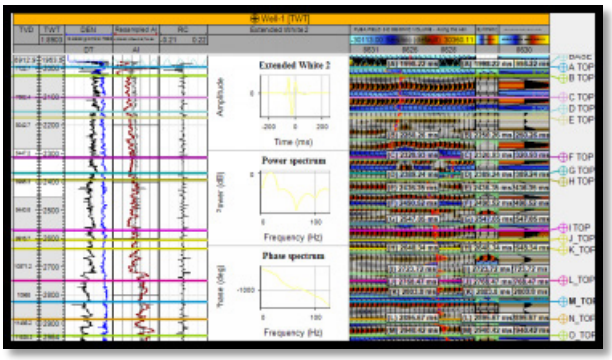

Figure 5: Synthetic seismogram generation and well-to-siesmic tie conducted for Fuba Field using Well-1 Checkshot

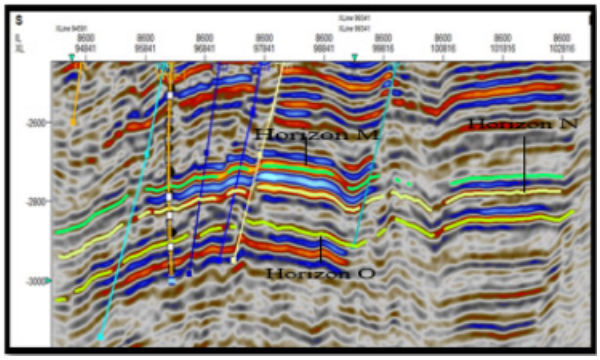

Figure 6: Faults and horizons interpreted along seismic inline section

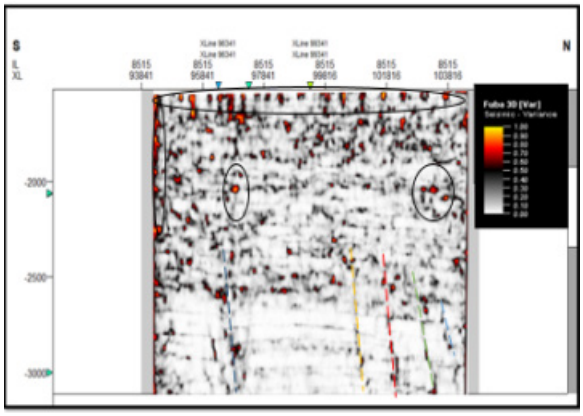

Figure 7: Variance Edge inline 8515

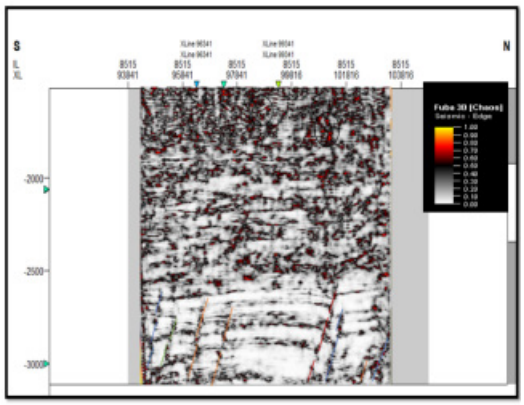

Figure 8: Chaos inline 8515

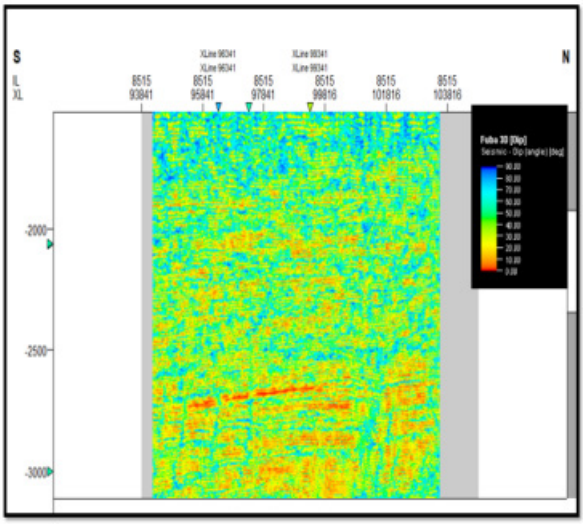

Figure 9: Dip Magnitude Inline 8515

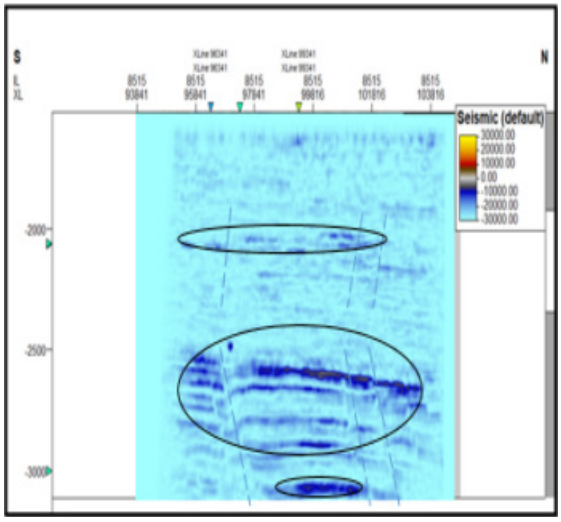

Figure 10: Sweetness inline 8515

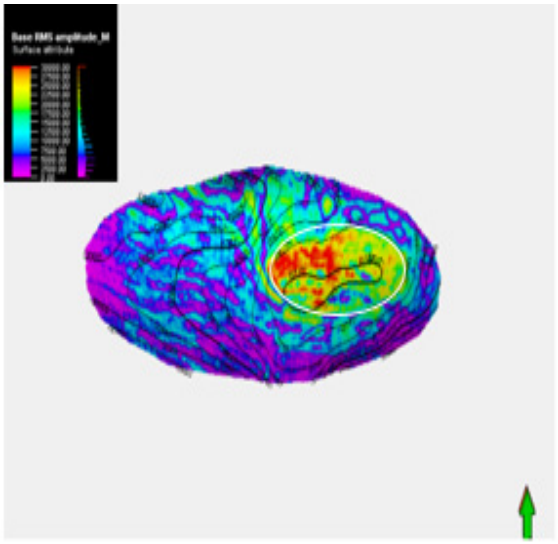

Figure 11: RMS amplitude map for Reservoir M

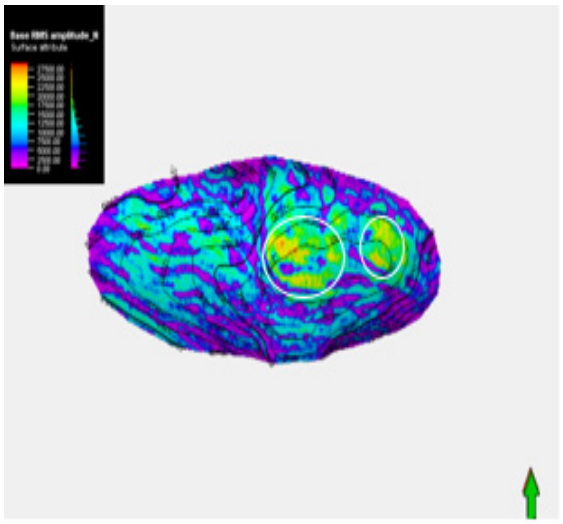

Figure 12: RMS amplitude map for Reservoir N

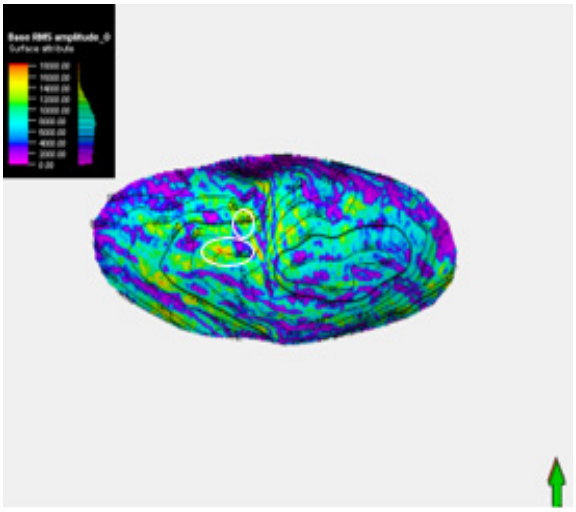

Figure 13: RMS amplitude map for Reservoir O

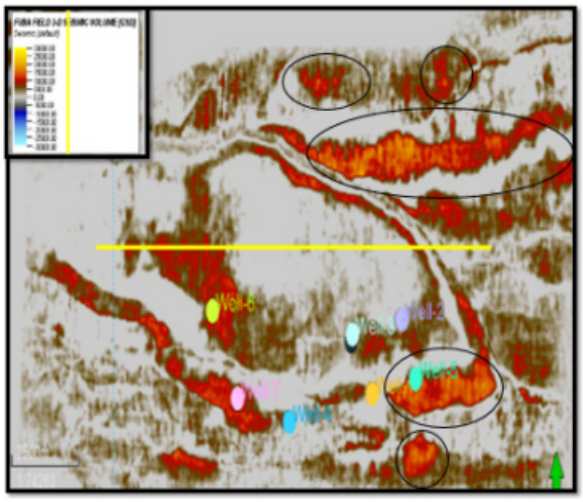

Figure 14: The General Spectral ecomposition Volume at Frequency of 12Hz to 35Hz

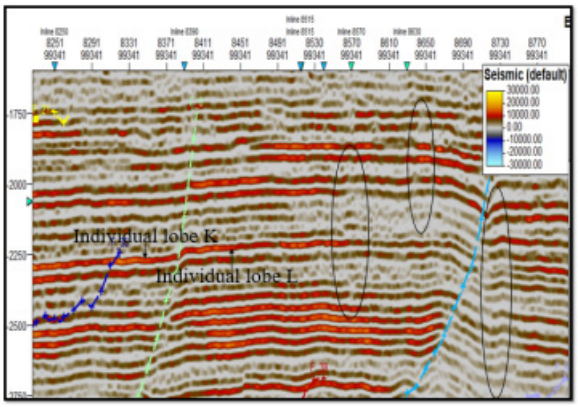

Figure 15: Seismic section of the stratigraphic contact showing unconformity

Table 1: RMS Amplitude Values for the Reservoir Surfaces

Reservoir	Range of RMS Amplitude Values
Reservoir-M	0 – 13,000
Reservoir _N	0 – 12,000
Reservoir _O	0 – 9,000

4.2: Well-to-Seismic Tie

The checkshot quality for Well-1 utilized for well-to-seismic tie is shown in Figure 4. The results for well-to-seismic tie conducted on Fuba field using density log, sonic log and checkshot of Well-1 is presented in Figure 5. An extended white 2 wavelet was used to give a near perfect match between the seismic and synthetic seismogram.

4.3: Fault and Horizon Interpretation

The results for the interpreted faults in Fuba field are presented in Figure 6 shows both synthetic and antithetic faults interpreted along seismic inlines. Faults are more visible along the inline direction because this direction reveals the true dip position of geologic structures. The variance time slice was used to validate the interpreted faults. All interpreted faults are normal synthetic and antithetic faults. A total of thirty-six faults were interpreted across the entire seismic data. Of the 36 interpreted faults, only F1 (synthetic fault) and F4 (antithetic fault) faults are regional, running from the top to bottom across the field. Hence, these faults play significant roles in trap formation at the upper, middle and lower sections of the field.

The results for the interpreted seismic horizons (Horizons M, N and O) are also presented in Figure 6. On these horizons, the fault polygons were generated and eliminated. The horizons were used as inputs for the generation of reservoir time surfaces.

4.4: Seismic Attributes

A series of seismic attributes such as variance edge, chaos, dip magnitude, sweetness, Root Mean Square (RMS) amplitude and spectral decomposition were generated in Petrel software interface to investigate potential structural and stratigraphic controls within the study area.

Figure 7 shows the computed variance attributes of the seismic section while Figure 8 shows the computed chaos attributes. The variance and the chaos values range from 0.0 to 1.0. Values of variance equal to 1 represent discontinuities while a continuous seismic event is represented by the value of 0. The high values are denoted with red to yellow colorations.

On the variance and the chaos maps, the areas dotted with blue, green, orange and pink colored lines signify values that correspond to the location of the discontinuity. The discontinuities may be interpreted as faults and boundaries as shown by the lines drawn on both attribute maps [21]. Both the variance edge and the chaos enhanced the faults or sedimentological bodies within the seismic data volume but the chaos enhanced the faults more. Furthermore, several bright spots are also delineated (in black circles and black ovals) which indicate high reflectivity sediments compared to their surroundings. These bright spots are an indication that a potential hydrocarbon trap might exist in the area. The darkest regions in the seismic section, which make vertical strips, may be interpreted as faults or fractures. The zones with low variance and chaos values are due to similar seismic traces. Areas with red patches represent lineaments/discontinuities while grey areas represent the structural framework of the field.

The variance attribute is edge imaging and detection techniques. It is used for imaging discontinuity related to faulting or stratigraphy in seismic data. Variance attribute is proven to help in imaging of channels, fault zones, fractures, unconformities and the major sequence boundaries [22].

Figures 9. shows the dip magnitude of the faults. The dip magnitude values range from 0 to 90. On Figure 9, the green colors represent areas of greater dip, while the red colors represent areas of shallower dip.

Figure 10. represents the sweetness values of the seismic data. The sweetness value ranges from 0 (blue) to 22,500 (yellow). High sweetness values may be attributed to both high amplitude and low frequency while low sweetness value is as a result of low amplitude and high frequency in the seismic volume.

The high sweetness regions within the seismic data (circled in black) indicate high amplitude. They are interpreted as hydrocarbon-bearing sand units. Though the sweetness attribute is effective for channel detection and characterization of gas-charged bearing sand units, it is known to be less effective when the acoustic impedance contrast between shale and sand units are low and when both lithology units are high. In most cases, shale intervals are characterized by low amplitude (low acoustic impedance contrasts) and high frequency thereby indicating low sweetness. Sand intervals are characterized by high amplitude (high acoustic impedance contrast with the shales) and low frequencies, thus indicating high sweetness values. Sweetness is used for identifying sweet spots that are hydrocarbon prone. The high sweetness values in the seismic section are possible indications of oil and gas [23-25].

The RMS amplitude was generated for all the studied reservoirs (reservoirs M, N and O). The result of the RMS amplitude analysis is presented in table 1 while Figures 11-13 show the RMS amplitude maps. The RMS amplitude values range from 0 (purple) to 13,000 (red) in reservoir M, from 0 (purple) to 12,000

(red) in reservoir N and 0 (purple) to 9,000 (red) in horizon O. The red-yellowish color represents hydrocarbon sands. Some of these hydrocarbon sands were not detected in the original seismic section. The observed changes may be due to changes in lithology or fluid content.

The RMS attribute is related to the variations in acoustic impedance. The higher the acoustic impedance values, the higher the RMS amplitude. The high values of RMS amplitudes may also be related to high porous sands, which are potential hydrocarbon reservoirs. RMS amplitude is similar to reflection strength and it is used in seismic exploration for delineating bright spots and amplitude anomalies [26-27]. The RMS amplitude is used for identifying coarser-grained facies, compaction related effects, and unconformities. The high values of RMS amplitudes circled (in white circles) in the maps are interpreted as high porosity lithologies, such as porous sands. These high RMS amplitude segments are potential high-quality hydrocarbon reservoirs.

The high amplitude (in white circles) in the seismic data conforms to the structures and confirm the presence of hydrocarbon [28]. The high amplitude ranges from light blue to yellow and red coloration. Root mean square amplitude is used as a good indicator of the presence of hydrocarbon in seismic data.

4.5: Spectral Decomposition

The general spectral decomposition was done at frequencies between 12Hz and 35Hz for the base and the monitor seismic. Figure 14 is the seismic volume obtained for the general spectral decomposition. Figure 14 illustrates Red-Green-Blue blend of the higher resolution of the frequency slices. The RGB colour blend effect gives a better understanding of the reservoirs geology. The colour blend is spectral balancing which recompense for wavelet and energy loss. The figure showed a complex meandering system and other less winding channels which are discontinuous and difficult to resolve on the seismic. The RGB colour blending slices revealed more hidden structures compared with what is observed in the time structural map. In this figure, the areas in red color indicate areas of low frequency and high amplitude associated with known hydrocarbon zones and when one colour is dominating, it showed that the frequency is dominating at that point. It revealed the geometry of the channels and other fewer sinusoidal channels. The channels are displayed with bright colouration which contains multiple frequencies as observed within the low frequency and indicated in black circles in Figure 14. The meandering channels run across from the north-eastern to the south-eastern part. These are likely traps for hydrocarbon accumulation. The amplitude response which is dominated by blue colour is high frequency. At the central part, there is high amplitude, an indication of hydrocarbon/gas effect. The acoustic impedance within the gas-bearing sand is lower compared to the surrounding shale [29]. At parts where there's a change in colour to brownish, it showed thickening up of the reflectors and greater contribution from the lower frequencies. There are colour changes in the channel system which could be indicative of changes in lithology.

4.6: Stratigraphic Contact

A major geologic feature was observed on the time-slice from the divergent pattern on the seismic section as we penetrate deeper, which is an unconformity (Figure 15). This represents a significant break in vertical velocity or breaks in deposition time or record on horizon [30]. This type of unconformity is called angular unconformity. Angular unconformity is an unconformity between two groups of rocks whose bedding planes are not parallel or in which the older underlying rock dips at a different angle (usually steeper) than the younger, overlying strata. Its interpretation depends on the recognition of characteristic reflection geometries rather than on amplitude information. It shows that deposition of the sediments took place at different times. Some of the lobes are indicated in Figure 15 (individual lobes K and L).

As can be seen in the areas in black ovals in Figure 15, the results of spectral decomposition at frequencies between 12Hz and 35Hz indicate the following: (a) There is more continuity of faults than previously interpreted; (b) The presence of small-scale faults in the field.

5.0: Conclusion

A total of four sand bodies (L, M, N and O) were identified and correlated across all seven wells in the field. All interpreted faults are normal synthetic and antithetic faults. A total of thirty-six faults were interpreted across the entire seismic data. Of the thirty-six interpreted faults, only F1 (synthetic fault) and F4 (antithetic fault) faults are regional, running from the top to bottom across the field. Hence, these faults play significant roles in trap formation at the upper, middle and lower sections of the field. Three horizons (M, N and O) were selected for the study. The seismic attributes interpreted include variance, chaos, dip magnitude, sweetness, root mean square amplitude and spectral decomposition. The variance and chaos values range from 0.0 to 1.0. The dip magnitude values range from 0 to 90 degrees. The variance, chaos and dip magnitude revealed the subtle structures and faults in the seismic section. The sweetness value ranges from 0 to 22,500. The RMS amplitude values range from 0 to 13,000 in the reservoirs. The RMS amplitude and sweetness results highlighted the hydrocarbon zones. The results of spectral decomposition indicate the following: (a) areas of low frequency and high amplitude associated with known hydrocarbon zones; (b) The presence of small-scale faults in the field; (c) The presence of channels and lobes in the field. The seismic attribute analysis in this study has helped in increasing the understanding of the delineated reservoirs and geological structures in the study area towards a better delineation of its hydrocarbon potential. Furthermore, it has been demonstrated that seismic attributes are complementary to the information derived through traditional methods of seismic interpretation. Hydrocarbon exploration and development risks can be reduced greatly with the outcome of seismic attributes extraction and analysis. It is recommended that 3-D seismic attributes for reservoir characterization of the studied field should be done for proper assessment and prospects definition of the area away from the area under well control.

Acknowledgements

The author is grateful to Shell Petroleum Development Company of Nigeria (SPDC), Port Harcourt Nigeria for the release of the academic data for the purpose of this study.

References

1. Liner C L (2004) Elements of 3D Seismology, 2nd Edition. PennWell Books, Tulsa, OK.
2. Oyeyemi K D, Aizebeokhai A P (2015) Seismic Attributes Analysis for Reservoir Characterization; Offshore Niger Delta. Petroleum and Coal 57: 619-628
3. Adewoye O, Amigun J O, Afuwai C G (2015) Lithostratigraphic Interpretation and Seismic Attributes Analysis for Reservoir Characterization in Some Parts of Niger Delta. Petroleum and Coal 57: 76-84.
4. Lefeuvre F E , Wrolstad K H, Zou K S, Smith L J, Maret J P, Nyein U K (1995) Sand-Shale Ratio and Sandy Reservoir Properties Estimation from Seismic Attributes: An Integrated Study. SEG Expand Abstracts 95: 108-110.
5. Omoja U C, Obiekezie T N (2019) Application of 3D Seismic Attribute Analyses for Hydrocarbon Prospectivity in Uzot-Field, Onshore Niger Delta Basin, Nigeria. International Journal of Geophysics 1-11.
6. Emujakporue O G, Enyenihi, E E (2020) Identification of Seismic Attributes for Hydrocarbon Prospecting of Akos field, Niger Delta, Nigeria. SN Applied Sciences 2: 910.
7. Ologe O, Olowokere T M (2021) Seismic Attributes Analysis as a Precursor to Hydrocarbon Indicators: A Case Study of "Ok" Field, Niger Delta. Tanzania Journal of Science, 47: 134-144.
8. Chen Q, Sidney S (1997) Seismic Attribute Technology for Reservoir Forecasting and Monitoring. Lead Edge 16: 445-448.
9. Pramanik A G, Singh V, Srivastava A K, Katiyar R (2002) Stratigraphic Inversion for Enhancing Vertical Resolution. Geohorizons 7: 8-18.
10. Van R P (2000) The Past, Present, and Future of Quantitative Reservoir Characterization. Leading Edge 19: 878-881.
11. Vig R., Singh V, Kharoo H L, Tiwari D N, Verma R P, Chandra M, Sen G (2002) Post Stack Seismic Inversion for Delineating Thin Reservoirs: A Case Study. In: Proceedings of 4th conference and Exposition in Petroleum Geophysics (Mumbai-2002) held during Jan 9: 287-291.
12. Chopra S, Marfurt K J (2005) Seismic Attributes—a Historical Perspective. Geophysics 70: 3-28.
13. Ochoma U (2023) Application of 3-D Seismic Attributes Analysis for Hydrocarbon Prospectivity in Onshore Fuba Field, Niger Delta, Nigeria. Asian Journal of Basic Science and Research 5: 83-96
14. Ayolabi E, Adigun A (2013) The Use of Seismic Attributes to Enhance Structural Interpretation in Z-Field, Onshore Niger Delta. Earth Science Research 1: 2.
15. Whiteman A (1982) Nigeria: Its Petroleum Ecology Resources and Potential. London, Graham and Trotman 394. http://dx.doi.org/10.1007/978-94-009-7361-9
16. Adegoke O S, Oyebamiji A S, Edet J J, Osterloff P L, Ulu O K (2017) Cenozoic Foraminifera and Calcareous Nannofossil Biostratigraphy of the Niger Delta. Elsevier, Cathleen Sether, United States.
17. Short K C, Stable A J (1967) Outline of Geology of Niger Delta. Bulletin of America Association of Petroleum Geologists 51: 761-779.
18. Horsfall O I, Uko E D, Tamunoberetonari I, Omubo Pepple V B (2017) Rock-Physics and Seismic-Inversion Based Reservoir Characterization of AKOS FIELD, Coastal Swamp Depobelt, Niger Delta, Nigeria. IOSR Journal of Applied Geology and Geophysics 5: 59-67.
19. Ochoma U, Uko E D, Horsfall O I (2020). Deterministic Hydrocarbon Volume Estimation of the Onshore Fuba Field, Niger Delta, Nigeria. IOSR Journal of Applied Geology and Geophysics 8: 34-40.
20. Cohen L (1989). Time-frequency Distributions-A Review. Proc. IEEE: 941-981.
21. Law W K, Chung A S C (2006) Minimal Weighted local variance as Edge detector For active contour models. In: Narayanan et al. PJ (eds), Accv , LNCS 3851: 622–632
22. Pigott J D , Kang M I H, Han H C (2013) First Order Seismic Attributes for Clastic Seismic Facies Interpretation: Examples from the East China Sea. Journal of Asian Earth Science 66: 34-54.
23. Hart B S, (2008) Channel Detection in 3-D Seismic Data Using Sweetness. AAPG Bulletin 92: 733-742.
24. Kosen S (2014) Enhancing Geological Interpretation with Seismic Attributes in Gulf of Thailand B.Sc report. Chula Long University, Thailand, 42.
25. Radovich B J, Oliveros R B (1998) 3-D Sequence Interpretation of Seismic Instantaneous Attributes from the Gorgon Field. Leading Edge, 17: 1286-1293.
26. Fozao K F, Fotso L, Djieto Lordon, A, Mbeleg M (2018) Hydrocarbon Inventory of the Eastern Part of the Rio Del Rey Basin Using Seismic Attributes. Journal of Petroleum Exploration and Production Technology 8: 655-665.
27. Opara A I, Osaki L J (2018) 3-D Seismic Attribute Analysis for Enhanced Prospect Definition of "Opu Field", Coastal Swamp Depo Belt Niger Delta, Nigeria. Journal of Applied Science, 18: 86-102.
28. Ajisafe Y C, Ako B D (2013) 3-D Seismic Attributes for Reservoir Characterization of 'Y' field, Niger Delta, Nigeria. IOSR Journal of Applied Geology andGeophysics 1: 23-31.
29. Naseer M T, Asim S (2017) Detection of Cretaceous Incised Valley Shale for Resource play, Miano gas field, SW Pakistan: Spectral Decomposition Using Continuous Wavelet Transform. Journal of Asian Earth Science 147: 358-377.
30. Neuendorf K K E, Mehl J P, Jackson J A (2005) Glossary of Geology, Fifth Edition. American Geological Institute, Alexandria, Virginia 779.